62-61

Reprinted from

CRYSTAL GROWTH

(Supplement to The Journal of Physics and Chemistry of Solids)

Proceedings of an International Conference on

Crystal Growth, Boston, 20–24 June, 1966

PERGAMON PRESS · OXFORD & NEW YORK · 1967

FAULT SURFACES IN ALPHA QUARTZ: THEIR ANALYSIS BY X-RAY DIFFRACTION CONTRAST AND THEIR BEARING ON GROWTH HISTORY AND IMPURITY DISTRIBUTION

A. R. LANG

H. H. Wills Physics Laboratory, University of Bristol, England

Abstract—X-ray topography has disclosed a variety of fault surfaces in quartz at which the regular lattice periodicity is disturbed and diffraction effects are produced similar to those from a stacking fault. The variation of fault diffraction contrast with indices of Bragg reflection provides data for the determination of fault vectors and hence for models of the fault structure. Fault vectors of Dauphiné and Brazil twin boundaries depend upon boundary orientation. Dauphiné twin boundaries are stepped on a fine scale. Fault surfaces other than twin boundaries may be parallel to growth horizons or they may transect them. Some fault surfaces coincide with boundaries of growth sectors. In synthetic quartz, fault surfaces are found in the boundaries of cells in regions of cellular growth.

INTRODUCTION

BOTH line defects and sheet defects in crystals can be studied by the diffraction contrast they produce, either with X-rays or electrons. The sheet defects observed by X-ray topography in quartz and other crystals include stacking faults, single twin boundaries, twin lamellae, and layers of crystal in which there is an anomalous interplanar spacing. Sheet defects can often be revealed by etching when they outcrop at natural or polished surfaces of the crystal; but such studies do not give as much information on the atomic structure of the defect as can be obtained from analysis of diffraction contrast, nor do they show the spatial disposition of the defects as readily as diffraction studies using transmitted radiation (especially X-rays). In this account of sheet defects in alpha quartz attention will be concentrated on those defects which, (1) only disturb the regular periodicity of the crystal over a distance much smaller than the X-ray extinction distance which is typically a few tens of microns, and (2) allow the lattices on either side of the defect to maintain parallelism with each other. Condition (2) excludes that common type of defect surface, the low-angle boundary, which is found in quartz as in other crystals. When the sheet defect is sufficiently localized as to satisfy condition (1) it may be replaced (as far as X-ray optics is concerned) by a single interface between two perfect regions of crystal. Such an interface we may call a *fault surface*, and, associated with it, we may define a *fault vector* which measures the displacement of the Bravais lattice on one side of the fault surface with respect to that on the other side. This is a realistic model for lattice defects associated with a sheet of impurity atoms one or a few atom layers thick, and it applies *a fortiori* to twin boundaries and to defects such as the "lattice disorders" discussed by MEGAW.[1]

Suppose a fault surface cuts through a perfect crystal in which dynamical equilibrium of incident and diffracted X-ray waves has been established. At the fault surface there arises "interbranch scattering" of waves between one branch of the dispersion surface and the other.[2] Its manifestation on the projection topograph[3] is a pattern of fringes parallel to the thickness contours of the crystal wedges which are enclosed between the fault surface and the specimen surfaces. The fringe period is related to that of the Pendellösung fringes seen in a single wedge-shaped crystal.[4] It was during the early X-ray topographic experiments on quartz[4,5] that types of fault surface previously unsuspected were brought to light. These pose intriguing questions, not only concerning the growth mechanisms of quartz and its mode of

incorporating impurity atoms into its structure, but also whether such faults may be of general occurrence in many crystal species. The recent observation of fault surfaces in ADP crystals is noteworthy.[6]

DETERMINATION OF FAULT VECTORS

The theory of fringes of the stacking-fault type is more complicated in the X-ray case[7] than in the electron case.[2,8] However, a simplified approach can be adopted when the fault vector is a small fraction of the interplanar spacing, for then a measure of the fault vector is provided by the mean excess diffracted intensity generated by the fault, averaged over the oscillations of the fringe pattern. There exists also the general condition for *invisibility* of the fault surface, that $\mathbf{g}\cdot\mathbf{f} = 2n\pi$ ($\mathbf{g}$ is the reciprocal lattice vector, $|g| = 2\pi/d_{hkl}$ for the reflection *hkl*, $\mathbf{f}$ is the fault vector, and n is zero or a positive or negative integer). A survey to find the reflections in which the fault surface is invisible, or nearly so, gives the value of $\mathbf{f}$ (subject to the ambiguities following from the above equation). It is worth noting that this survey is more easily accomplished with X-rays than with electrons since in the X-ray case definitely only one reflection *hkl* is excited in the production of each topograph, and the comparison of topographs of successive orders of reflection from a given Bragg plane enables the $\mathbf{f}$-component normal to that plane to be established to an accuracy of a few per cent. Since the two common forms of twinning in quartz (i.e. Brazil and Dauphiné) are of the parallel-lattice type, it follows that their boundaries may be studied as fault surfaces obeying condition (2) above. In deriving the fault vectors at twin boundaries, attention must be paid to the phase of the X-ray reflection concerned, since quartz is a non-centric structure. Thus, at a twin boundary at which the structure amplitude changes from $F\exp(-i\phi)$ to $F\exp(+i\phi)$ and a Bravais lattice displacement $\mathbf{f}$ is encountered on crossing the boundary, the condition for invisibility of the boundary becomes* $\mathbf{g}\cdot\mathbf{f}+2\phi = 2n\pi$. However, reflections from planes in a zone whose axis is one of the two-fold axes of the structure have $\phi = 0$ or π with respect to an origin on that two-fold axis (see Fig. 1). The Dauphiné twin law is a rotation of π about the c-axis. Consequently, the only planes in the $\langle 11\bar{2}0\rangle$ zones which are structurally equivalent on either side of the twin boundary are (0001) and

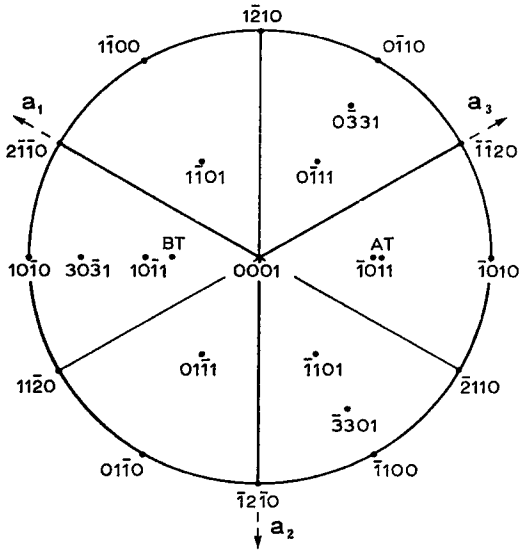

FIG. 1. Stereographic projection parallel to the c-axis showing poles of the chief planes used in X-ray topographic surveys. The two-fold axes are parallel to the a-axes and pierce the structure at heights which depend upon the hand of the structure.

$\{10\bar{1}0\}$: for these alone the simple invisibility rule $\mathbf{g}\cdot\mathbf{f} = 2n\pi$ applies. With other planes in these zones, and indeed all other planes except those in $\langle 10\bar{1}0\rangle$ zones, interbranch scattering at the twin boundary will arise from the change in structure factor *moduli*. On the topograph the obvious manifestation of this change is a difference in diffracted intensity from crystal volumes on either side of the boundary.[9] In Brazil twinning, on the other hand, the twin law is a reflection in a plane normal to a two-fold axis, and different rules apply to each of the $\langle 11\bar{2}0\rangle$ zones. When the composition plane contains a two-fold axis, which is commonly the case, it is structurally reasonable to place the Bravais lattice origin on that two-fold axis, on both sides of the twin boundary. Then for reflections from the $\langle 11\bar{2}0\rangle$-type zone which contains the composition plane, the invisibility rule is $\mathbf{g}\cdot\mathbf{f} = 2n\pi$; for the other $\langle 11\bar{2}0\rangle$ zones it is $\mathbf{g}\cdot\mathbf{f}\pm 2\pi/3 = 2n\pi$. Assessment of fault vectors from

* Note that ϕ changes sign when $\mathbf{g}$ does, and that when Friedel's law is obeyed $\phi(\mathbf{g}) = -\phi(\bar{\mathbf{g}})$.

the strength of fault images is necessarily somewhat subjective: it is hoped that X-ray moiré fringes may provide a more direct method of measurement.[10]

OBSERVATIONS ON NATURAL QUARTZ

Figure 2 shows part of a plate of natural quartz. Practically the whole field is covered by fine bands that delineate growth horizons. Such stratifications are detectable with great sensitivity by X-ray topographic methods, and with the aid of a double-crystal spectrometer technique[11] the lattice inclinations and tilts associated with them can be measured. The geometry of the pattern of Fig. 2 can be understood by reference to Figs. 1 and 3. Parts of three growth sectors are covered in the topograph, two major rhombohedral (r) and one minor rhombohedral (z). Wedges of Brazil-twinned material are present. They are bounded by the planes (Br) and (Bm): discussion of these boundaries is deferred until the following section. The intense black lines are dislocations. Some of them are decorated and some are helical. In the bottom right corner of the field the diffraction contrast by growth stratifications (here parallel to $(\bar{1}101)$) is locally quite intense, and at certain horizons the change in interplanar spacing is sufficiently abrupt to cause interbranch scattering strong enough to show fault fringes distinctly.

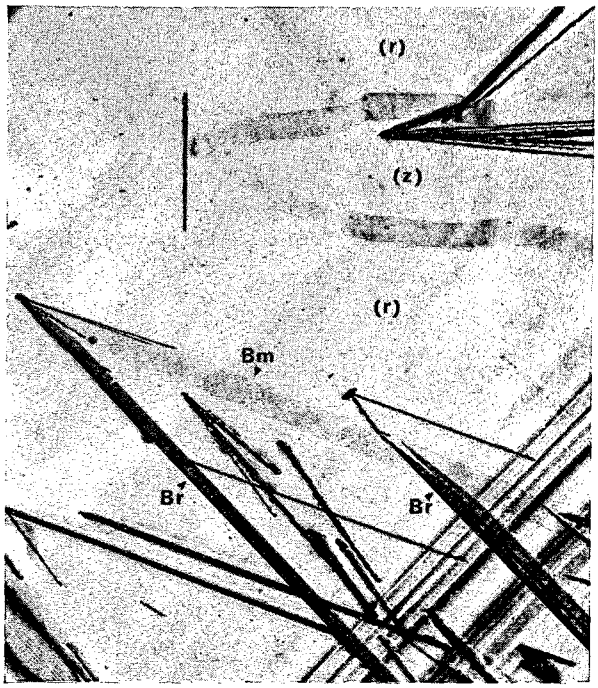

FIG. 2. Topograph of natural quartz plate inclined 11° to major rhombohedron $(10\bar{1}1)$. Thickness 1 mm. Reflection $10\bar{1}\bar{1}$, Ag$K\alpha$ radiation. Field area $1 \times 1{\cdot}3$ mm. Marked features explained in text. Plate is viewed along a direction tilted 40° away from the c-axis towards the normal to $(10\bar{1}1)$. Projection of diffraction vector is horizontal, direction $[\bar{1}2\bar{1}0]$ is vertical on the topograph.

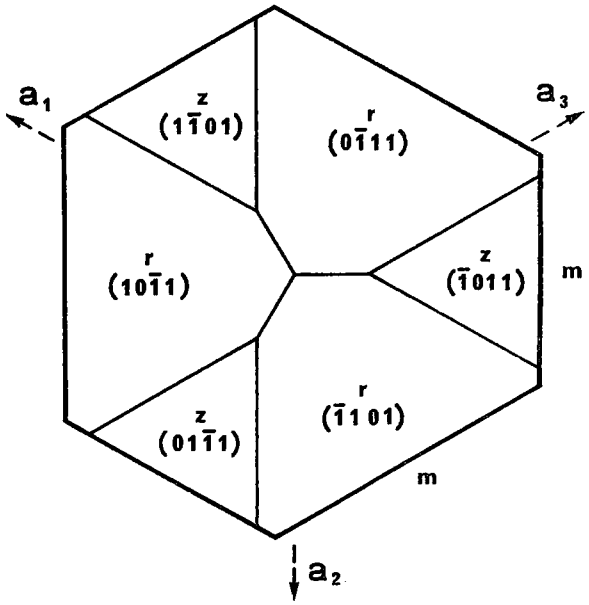

FIG. 3. Idealized section of a quartz crystal cut parallel to the basal plane showing division into major and minor rhombohedral growth sectors. Traces of r–z growth sector boundaries are parallel to $\{10\bar{1}0\}$ and r–r to $\{11\bar{2}0\}$. Growth layers parallel to r and z faces would outcrop with traces parallel to the sides of the hexagon, i.e. to $\{10\bar{1}0\}$.

Careful observation may be necessary to distinguish between a set of such fringes due to strong scattering at a single horizon, and the individual images of a set of regularly spaced growth strata each producing only weak scattering. The distinction can be made on section topographs[12] by reference to particular features of the fringe patterns that appear in such topographs.[7] Even when the strain gradients in the growth layers are too low to produce increased diffracted intensity through interbranch scattering, they may still be detected by the bending of Pendellösung fringes they produce in the section-topograph Pendellösung fringe pattern.[13,14]

Various fault surfaces transect growth horizons. One type has a simple topographic rationale: they lie in the boundaries of growth sectors. These sector-boundary fault surfaces have only been observed in crystals which also show growth stratifications. It may be that they develop only above a certain impurity concentration. Figure 2 shows a fairly weak fringe pattern due to a fault surface between the *r* and *z* growth sectors. In no Bragg reflection from this specimen do fault-surface fringes appear in the *r*–*r* sector boundary located above the *z* sector in the figure. The best-developed fringe patterns are often exhibited by fault surfaces whose nature is at present little understood. They are not identifiable as twin boundaries, though the possibility exists that some of them may contain thin twin lamellae. They may be flat or they may be irregular. Some flat surfaces are describable only by high indices. A rough division may be made into "strong" and "weak" surfaces. The "strong" surfaces give rise to an excess diffracted intensity in addition to that pertaining to the fringe system. This excess appears due to lattice curvature where the fault surface outcrops the surfaces of the specimen plate. Such curvature arises from the relief of stress within the fault surface. In the bottom left-hand corner of Fig. 2 a short segment of such a surface is seen. At the other extreme, the most "weak" surfaces are those that are revealed only in high-order Bragg reflections. Intermediate are surfaces such as are illustrated in Fig. 4. These show a distinct but complicated fringe pattern in low-order reflections; but in certain high-order reflections they manifest strong excess diffracted intensity due to long-range lattice strains. Some strong fault surfaces are rapidly etched out by hydrofluoric acid or hot strong alkali. The surfaces in Fig. 4 were not revealed by etching in HF. A possible explanation of fault surfaces that are not twin or growth sector boundaries is that they mark boundaries of parallel crystal growths, including growths that have become enveloped in the main crystal.

TWIN BOUNDARY STRUCTURES

Crystal volumes related by the Brazil twin law can be differentiated topographically with the aid of anomalous dispersion of X-rays which produces conditions such that Friedel's law is no longer obeyed;[9] but for the purpose of determining twin boundary fault vectors it is simpler to use radiations such as Mo$K\alpha$ and Ag$K\alpha$ which are far removed from the silicon K absorption edge. It is known that traces of Brazil twin boundaries outcropping on crystal surfaces are usually straight whereas those of Dauphiné boundaries are irregularly curved.[15] This macroscopic difference has been confirmed by X-ray topography. Projection topographs of Brazil twin boundaries in oscillator-grade quartz show them to be flat and oriented parallel to low-index planes. If steps on a fine scale are distributed over the Brazil twin boundaries studied then they occur on a smaller scale than can be resolved by X-ray topography (less than about a micron in height). In the case of Dauphiné twin boundaries the situation is quite different. Topographs reveal that Dauphiné twin boundaries lying in certain mean orientations are stepped on a very fine scale, down to the topographic resolution limit (see Fig. 5). This fine structure is not described

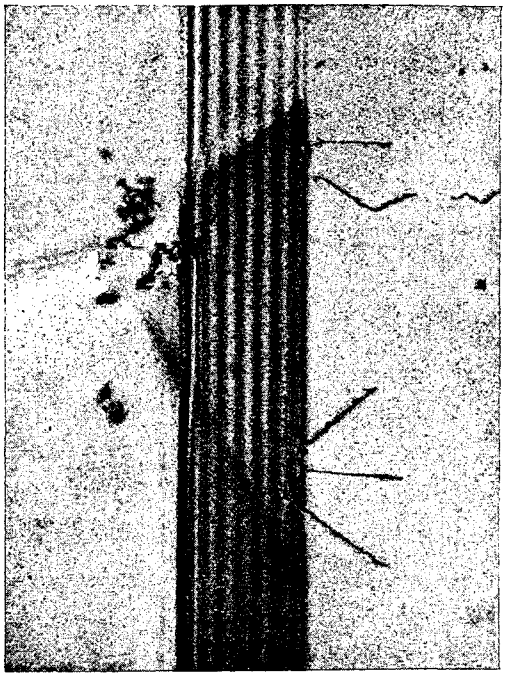

FIG. 4. Detail of flat fault surfaces intersecting a natural quartz plate 0·3 mm thick. Plate orientation 3° off ($\bar{1}011$). Fault surfaces whose trace is vertical are parallel to ($\bar{1}010$). Width of trace on topograph is 0·3 mm. Six dislocation images are seen on right of fault surface, curved and decorated dislocations appear on left.

in the standard works of reference. Indeed, twin boundary steps on the scale of a micron or two would escape notice in the usual method of delineating twin boundaries by etching crystal surfaces.

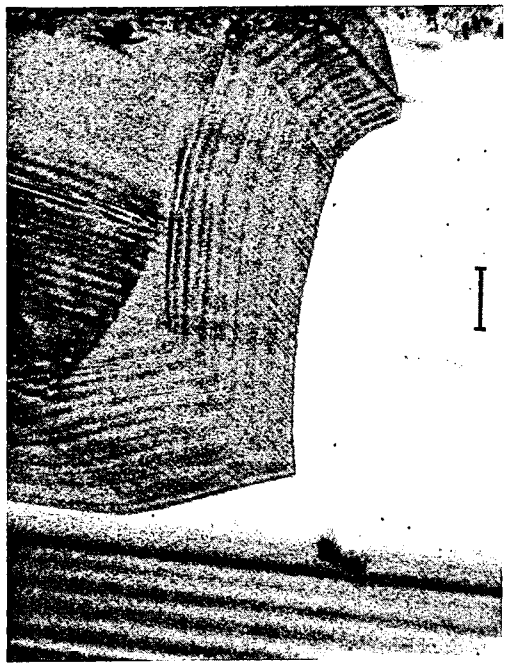

FIG. 5. Fine structure of Dauphiné twin boundary intersecting a natural quartz plate 1 mm thick. Major rhombohedral plane is Bragg reflecting on left of boundary, minor rhombohedral plane on right. Bands in lowest part of field are growth stratifications. Dark area near left margin is a crack. Twin boundary shows both fault fringes parallel to depth contours and also fine steps. Scale mark 50 microns.

Regarding fault vectors, it has been found that these depend upon the orientation of the boundary surface, both with Brazil and Dauphiné twinning. In the latter twinning, this dependence may be strikingly evident. At a stepped Dauphiné twin boundary, diffraction contrast from one of the step surfaces may be strong and from the other be zero, in a given Bragg reflection. In the basal-plane reflections, 0003 and 0006, diffraction contrast from Dauphiné twin boundaries in all orientations is very weak or zero. In Fig. 2 the Brazil twin boundaries (*Br*) parallel to $(0\bar{1}11)$ show stronger contrast than the boundary (*Bm*) parallel to $(01\bar{1}0)$. (*Br*) vanish in the 0003 reflection: (*Bm*) do not.

In a recent electron microscope study, MCLAREN and PHAKEY[18] have investigated the fault vector at Brazil twin boundaries in amethyst quartz lying parallel to the major rhombohedron.* They find its direction to lie parallel to the two-fold axis in the composition plane, and its magnitude to be equal to half the basal-plane lattice translation. X-ray topographs of good quality quartz confirm this direction of fault vector, but find its magnitude to be less than $\frac{1}{2}a_0$, being probably about $0{\cdot}4a_0$.

FAULT SURFACES IN SYNTHETIC QUARTZ

In synthetic quartz there is found a type of fault surface that is topographically understandable. It occurs in regions where the crystal has grown on a surface roughly parallel to (0001). The fault surfaces divide the crystal into cells a few millimeters in diameter and are clearly associated with the mode of cellular growth that gives rise to a rough external crystal surface known as the "cobble" texture.[19] X-ray topographs of slices cut parallel to (0001) which include some of the final cobbled surface of the crystal indicate that the fault surfaces lie in the boundaries between growth cells, and they consequently outcrop at the crystal surface at the grooves between cobbles. Since it is known that the degree of development of the cobble structure is proportional to the amount of aluminium impurity present, it is reasonable to suppose that the anomalous interplanar spacings that produce the fault surfaces in the cell boundaries are due to a local high concentration of aluminium impurity, possibly forming an ordered boundary structure. There is a tendency for dislocations to lie in, or close to, the fault surfaces, but their frequency of occurrence in the fault surface may be as low as one dislocation per several tens of microns.

REFERENCES

1. MEGAW, H. D., *Proc. Roy. Soc.* A **259**, 59 (1960).
2. HIRSCH, P. B., HOWIE, A., NICHOLSON, R. B., PASHLEY, D. W. and WHELAN, M. J., *Electron Microscopy of Thin Crystals*, Butterworths, London (1965).

* Note that these authors' Miller-Bravais axes are not oriented according to the mnemonic[16] they cite, because they have labelled the right-handed structure with the left-handed space group symbol,[17] and vice versa.

3. LANG, A. R., *Acta Cryst.* **12,** 249 (1959).
4. KATO, N. and LANG, A. R., *Acta Cryst.* **12,** 789 (1959).
5. LANG, A. R., *J. Appl. Phys.* **30,** 1748 (1959).
6. YOSHIMATSU, M., *Jap. J. Appl. Phys.* **5,** 29 (1966).
7. KATO, N., USAMI, K. and KATAGAWA, T., *Proceedings of Fifteenth Annual Conference on Applications of X-ray Analysis*, Denver, 1966 (to be published).
8. WHELAN, M. J. and HIRSCH, P. B., *Phil. Mag.* **2,** 1121, 1303 (1957).
9. LANG, A. R., *Appl. Phys. Lett.* **7,** 168 (1965).
10. LANG, A. R. and MIUSCOV, V. F., *Appl. Phys. Lett.* **7,** 214 (1965).
11. BONSE, U. F., *Z. Physik.* **184,** 61 (1965).
12. LANG, A. R., *Acta Met.* **5,** 358 (1957).
13. KATO, N., *Acta Cryst.* **14,** 526, 627 (1961); *J. Phys. Soc. Jap.* **18,** 1785 (1963); **19,** 67, 971 (1964).
14. HART, M., *Appl. Phys. Lett.* **7,** 96 (1965).
15. FRONDEL, C., *Dana's System of Mineralogy*, 7th Edition, Vol. III, Wiley, New York (1962).
16. LANG, A. R., *Acta Cryst.* **19,** 290 (1965).
17. HENRY, N. F. M. and LONSDALE, K., *International Tables for X-ray Crystallography*, Vol. I, Kynoch Press, Birmingham (1965).
18. MCLAREN, A. C. and PHAKEY, P. P., *Phys. Stat. Sol.* **13,** 413 (1966).
19. BROWN, C. S. and THOMAS, L. A., *J. Phys. Chem. Solids* **13,** 337 (1960).